


RESEARCH

Open Access



The assessment of climatic, environmental, and socioeconomic aspects of the Brazilian Cerrado

Washington Luiz Félix Correia Filho¹, José Francisco de Oliveira-Júnior^{2,3}, Dimas de Barros Santiago⁴, Hazem Ghassan Abdo^{5,6,7*} , Hussein Almohamad⁸, Ahmed Abdullah Al Dughairi⁸ and Carlos Antonio da Silva Junior⁹

Abstract

Background The Cerrado is the most biodiverse savanna and maintains other biomes. Aware of its significance, this paper evaluated the Brazilian Cerrado's climatic, environmental, and socioeconomic aspects using remote sensing data and spatial statistics (correlation analysis and principal components analysis—PCA). Following the measures of sample adequacy (MSA) and Kaiser–Meyer–Olkin (KMO) tests, seventeen variables were evaluated.

Results The MSA revealed that the dataset had a good quality (0.76), and nine variables were selected: elevation, evapotranspiration, active fires, Human Development Index (HDI), land use and land cover (LULC; shrubland and cropland/rainfed), rainfall (spring and autumn), and livestock. The correlation matrix indicated a positive (negative) association between HDI and autumn rainfall (HDI and active fires) with a value of 0.77 (–0.55). The PCA results determined which three principal components (PC) were adequate for extracting spatial patterns, accounting for 68.02% of the total variance with respective values of 38.59%, 16.89%, and 12.5%. Due to economic development and agribusiness, Cerrado's northern (central, western, and southern) areas had negative (positive) score HDI values, as shown in PC1. Climatic (rainfall—spring and fall) and environmental (cropland/rainfed and shrubland) aspects dominated the PC2, with negative scores in northern and western portions due to the transition zone between Amazon and Cerrado biomes caused by rainfall variability. On the other hand, environmental aspects (LULC-shrubland and elevation) influenced the PC3; areas with high altitudes (> 500 m) received a higher score.

Conclusion Agricultural expansion substantially affected LULC, leading to deforestation-caused suppression of native vegetation.

Keywords Environment, Agribusiness, Active fire, Human Development Index, Land use and land cover

*Correspondence:

Hazem Ghassan Abdo

hazemabdo@tartous-univ.edu.sy

Full list of author information is available at the end of the article



© The Author(s) 2023. **Open Access** This article is licensed under a Creative Commons Attribution 4.0 International License, which permits use, sharing, adaptation, distribution and reproduction in any medium or format, as long as you give appropriate credit to the original author(s) and the source, provide a link to the Creative Commons licence, and indicate if changes were made. The images or other third party material in this article are included in the article's Creative Commons licence, unless indicated otherwise in a credit line to the material. If material is not included in the article's Creative Commons licence and your intended use is not permitted by statutory regulation or exceeds the permitted use, you will need to obtain permission directly from the copyright holder. To view a copy of this licence, visit <http://creativecommons.org/licenses/by/4.0/>.

Introduction

Similar to other Brazilian biomes, the Brazilian Cerrado has undergone several transformations in recent decades (Silva et al. 2013; Silva Junior et al. 2018). Such changes can have climatic (Durigan and Ratter 2016; Mataveli et al. 2018; Correia Filho et al. 2019), environmental (Sano et al. 2020; Oliveira et al. 2021), and human causes based on the rapid changes in land use and cover (Hunke et al. 2015; Dias et al. 2016; Soterroni et al. 2019; Souza et al. 2020a, b). In addition, the central-southern portion of the Cerrado has also experienced landscape and land-use changes due to the expansion of agribusiness (Dias et al. 2016; Salazar Pessôa 2020).

The concept of agribusiness emerged in the mid-1960s and 1970s after the deployment of the National Development Programs (in Portuguese, *Programas Nacionais de Desenvolvimento*, PND) by the Brazilian Federal Government to modernize and expand regional based on agricultural production (Salazar Pessôa 2020). These PNDs had the support of the Brazilian Agricultural Research Corporation (in Portuguese, *Empresa Brasileira de Pesquisa Agropecuária*, EMBRAPA), which is responsible for the genetic improvement process of grain production (Silva et al. 2013; Souza et al. 2020b).

This PND in the Cerrado was started in the late 1970s with the Japanese–Brazilian Cooperation Program for the Development of the Cerrado (in Portuguese, *Programa de Cooperação Nipo-Brasileiro para o Desenvolvimento Agrícola dos Cerrados*, PROCEDER), which lasted until 2001 (Silva et al. 2013; Buainain and Garcia 2015; Salazar Pessôa 2020). Over the past three decades, PROCEDER contributed to the growth and development of agribusiness by raising agricultural productivity and enhancing the Brazilian trade balance (Picoli et al. 2020; Salazar Pessôa 2020; Souza et al. 2020b). Consequently, the center-south portion of the Cerrado has become a significant producer of commodities, supplying Brazil and the rest of the globe (da Silva et al. 2013; Soterroni et al. 2019; Salazar Pessôa 2020).

This program established a second agricultural frontier in the mid-1990s, located in the states of Maranhão–Tocantins–Piauí–Bahia (MATOPIBA) through the expansion of soybean cultivation (Buainain and Garcia 2015; Souza et al. 2020a, b). In contrast, this development based on extensive land use due to mining, cattle ranching, and agricultural consortia causes a series of environmental degradations in the Cerrado (Cunha et al. 2008), most notably the suppression of native vegetation on 7340 km² by 2020 (Hunke et al. 2015; Garcia and Ballester 2016; Silva Junior et al. 2019; Souza et al. 2020a, b).

If soybean cultivation's current agricultural expansion persists over the Cerrado biome, approximately 2.5 million hectares of the native landscape will undergo

significant changes by 2050 (Soterroni et al. 2019). In addition, deforestation is an environmental degradation more common (Rocha et al. 2011; Santos et al. 2014; Mataveli et al. 2018; Souza et al. 2020b; Assis et al. 2021), associated with clearing and fire-related agricultural expansion in some states as Maranhão (Silva Junior et al. 2019; Oliveira et al. 2021), Minas Gerais (Rudorff et al. 2010; Marinho et al. 2021).

Despite the vital role of fire in the renovation and growth of plants (Durigan and Ratter 2016; Abdo 2018; Abdo et al. 2022), however, most of the wildfires originating over the biome arise from human actions (Mataveli et al. 2018; Silva Junior et al. 2019). Concern exists regarding Cerrado's ability to support endemic fauna and flora (Durigan and Ratter 2016; Garcia and Ballester 2016; Abreu et al. 2017). Alves and Rosa (2019) highlight Cerrado's significance in forming the leading Brazilian rivers, given Brazil's dependence on hydroelectricity (Goldemberg and Lucon 2007). The Cerrado is also responsible for maintaining other biomes and is the most biodiverse savanna (Valadão et al. 2017).

Aware of the deficiency of a broader assessment that seeks to know how different aspects interact over the Brazilian Cerrado, the primary objective of this study is to evaluate the Brazilian Cerrado's climatic, environmental, and socioeconomic aspects.

Materials and methods

Study area

The Cerrado biome is located in the Brazilian Central Plateau, covering 24% of Brazil (2.06 million km² of total area) with the second largest biome in Brazil, ranging from open grasslands to dense forest formations (Becerra et al. 2009; Valadão et al. 2017). The Cerrado area comprises the following states: Amapá, Bahia, Ceará, Distrito Federal, Goiás, Maranhão, Minas Gerais, Mato Grosso, Mato Grosso do Sul, Pará, Paraná, Piauí, Rondônia, Roraima, São Paulo, and Tocantins, totaling 1445 municipalities (Grupo de Trabalho Biomas do Cerrado 2004), as seen in Fig. 1.

The Cerrado has a seasonal tropical climate, with dry winters and an average annual temperature between 22 and 23 °C, with highs exceeding 40 °C and lows approaching negative values (between May and July) (Nascimento and Novais 2020). The average annual rainfall varies between 1200 and 1800 mm, particularly during spring and summer (October and March). However, there is no monthly rainfall during the austral autumn and winter (May and September) (Nascimento and Novais 2020; Correia Filho et al. 2022a). Therefore, three datasets were used to assess the climatological, environmental, and socioeconomic aspects of the Brazilian Cerrado:

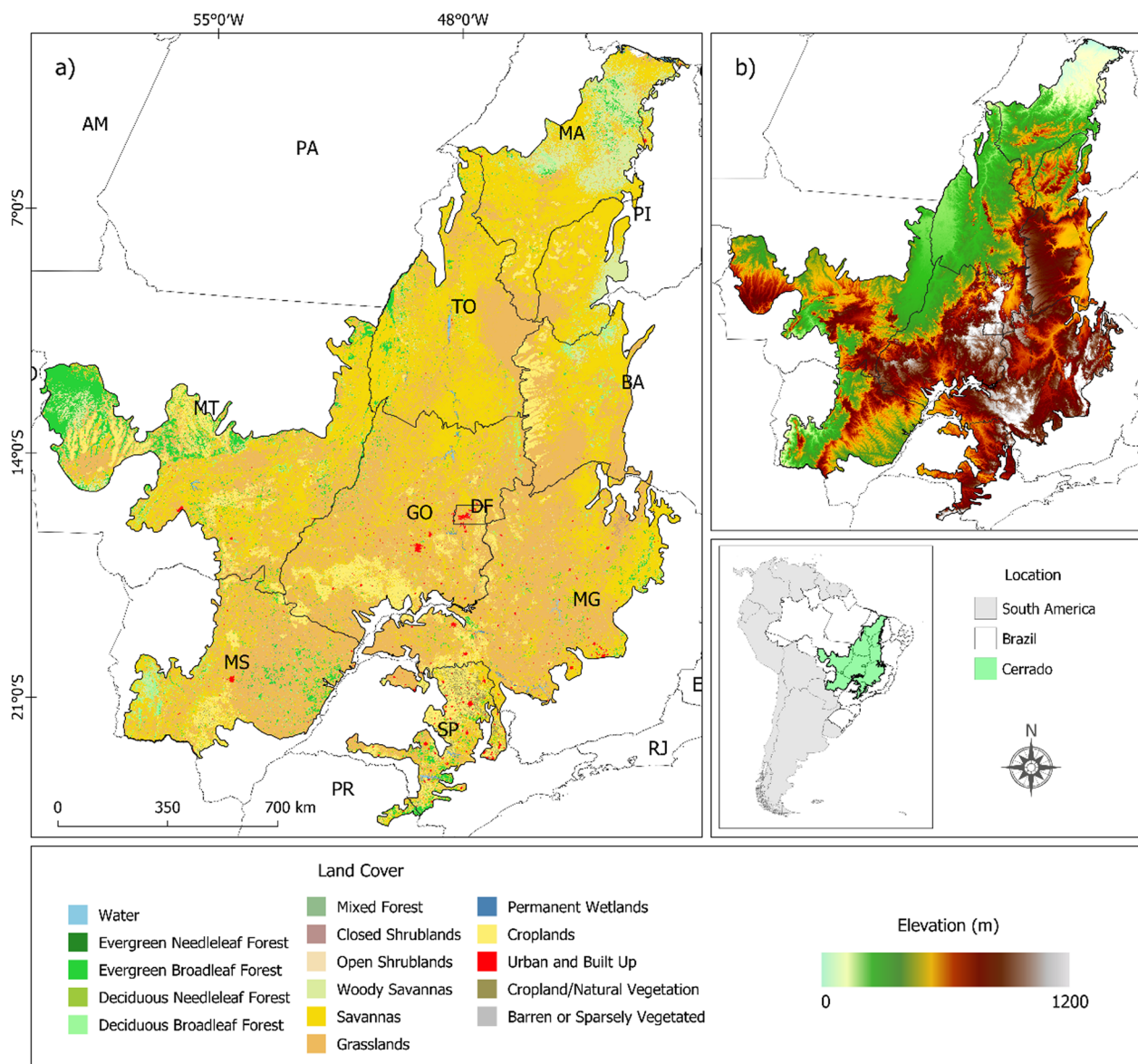


Fig. 1 Delimitation of the Cerrado biome, located in the central South America (middle right panel), classified into **a** 16 land use and land cover classes (top and bottom left side) (Bontemps et al. 2015, ESA 2021); and **b** elevation (top right panel, unit: meters) which spans from 0 to 1200 m (bottom right panel) (Jarvis et al. 2008)

- Climatological (rainfall, temperature, and evapotranspiration);
- Environmental (active fires, elevation, vegetation health index, slope, and land use and land cover—LULC);
- Socioeconomic (actual yield production, gross domestic production—GDP, Human Development Index—HDI, population density, and livestock).

Climatological data

To assess the climatic, environmental, and socioeconomic aspects of the Brazilian Cerrado, we will begin by obtaining rainfall data. It used the second version of the Climate Hazard Group InfraRed Precipitation with Station (CHIRPS) for rainfall product (unit: mm) (Funk et al. 2015a). This product’s information is derived from satellite products, weather stations, and reanalysis data. In addition, it has a spatial resolution of 0.05° × 0.05°, and temporal resolution on daily, pentad, and monthly scales is applicable between the latitudes of 60° N and 60° S and

is available through the website <ftp://ftp.chg.ucsb.edu/pub/org/chg/products/CHIRPS-2.0>. The CHIRPS data are consistent in regions with high station density (Funk et al. 2015b), particularly in Brazil, as confirmed by Costa et al. (2019), Oliveira-Júnior et al. (2021), and Palharini et al. (2021), and Correia Filho et al. (2022a) who recently used it as a reference in remote regions or regions with poor or absent rain gauge coverage. This study calculated the seasonal averages from 1982 to 2021: (a) spring, (b) summer, (c) fall and (d) winter.

Regarding evapotranspiration data (unit: kg/m^2 , but similar to mm), the sixth version of the MOD16A2 product from the moderate resolution imaging spectro-radiometer (MODIS) sensor of the Terra Satellite was utilized (Running et al. 2017). This product has a spatial resolution of $500 \text{ m} \times 500 \text{ m}$ and a weekly and annual temporal resolution. For this study, it was calculated the average annual from 2001 to 2021.

Land surface temperature (LST, unit: Kelvin) products were acquired by polar-orbiting satellites using the advanced very high-resolution radiometer (AVHRR) sensor, which is operated by the National Oceanic and Atmospheric Administration (NOAA). This product is part of the initiative for the Global Vegetation Health (GVH) program that evaluates the behavior of terrestrial vegetation using the Normalized Difference Vegetation Index (NDVI) and the Vegetation Health Index (VHI). The data have a spatial resolution of $0.04^\circ \times 0.04^\circ$, and weekly temporal resolution has been available since 1981 (Kogan et al. 2011). In this instance, the temperature estimation derived from the cloud-top brightness temperature algorithm pertains to LST, not air temperature. For this study, the average annual LST corresponds to 1982–2021.

Environmental data

In addition to the LST, NOAA provided the Vegetation Health Index (VHI, unit: %) from the Global Vegetation Health program, which has a spatial resolution of $0.04^\circ \times 0.04^\circ$ and temporal resolution on a weekly VHI scale to assess the vegetative health and ranges from 0 to 100. The average annual VHI for the study spans from 1982 to 2021 (Karnieli et al. 2010; Kogan et al. 2011).

About the LULC data, it used version 2.0.7 of the Space Agency—Climate Change Initiative—Land Cover (ESA CCI-LC)—(Bontemps et al. 2015, ESA 2021), with a spatial resolution of $300 \text{ m} \times 300 \text{ m}$ with temporal resolution in annual scale, corresponding to the period of 1990–2015, which were derived from the SPOT-VEGETATION (1999–2012), and PROBA-V (2013–2015) satellites. In this study, the two most abundant groups of LULC were utilized for evaluation: cropland/rainfed and shrubland, relative to the 2015 year.

The active fire data were obtained from BDQueimadas of the *Divisão de Satélites e Sistemas Ambientais* (DSA) at the Center for Research in Weather and Climate Studies/Brazilian Institute of Space Research (CPTEC/INPE 2019). This product is generated from the number of recordings of potential fire events detected by orbital and geostationary satellites between 2003 and 2021 and documented annually in .csv files. First, this study converted the .csv files to GeoTIFF files with a spatial precision of $0.05^\circ \times 0.05^\circ$. After this step, the annual average for this period was then calculated.

The slope data (unit: $^\circ$) were from the third version of the Global Agro-Ecological Zones (GAEZ) program, developed by the International Institute for Applied Systems Analysis (IIASA) and the Food and Agriculture Organization (FAO)—(IIASA/FAO 2012). The elevation data (unit: meters) were collected from version 2.1 of the Shuttle Radar Topography Mission (SRTM) elevation model, which has a spatial resolution of $90 \text{ m} \times 90 \text{ m}$ and covers the whole globe between latitudes 60° N and 60° S (Jarvis et al. 2008).

Socioeconomic data

For socioeconomic data, Population Density, Human Development Index (HDI), and Gross Domestic Product (GDP) used the year 2015 as a basis (Kummu et al. 2018). This item has a spatial resolution between $0.01^\circ \times 0.01^\circ$ and $0.25^\circ \times 0.25^\circ$. Similar to the slope data, the livestock and actual yield and production variables from the third version of the Global Agro-Ecological Zones (GAEZ) program, developed by the International Institute for Applied Systems Analysis (IIASA) and the Food and Agriculture Organization (FAO)—(IIASA/FAO 2012), with a spatial resolution of $0.08^\circ \times 0.08^\circ$. The entire base was normalized and transformed to a spatial resolution of 0.05° using R software version 4.0-4 and the bilinear interpolation method (R Development Core Team 2021). Each examined variable corresponds to the average annual composition (climatic and environmental variables) or Census (socioeconomic variables).

Table 1 Pearson correlation analysis classification

Interval	Intensity
0.0–0.3	Negligible
0.3–0.5	Poor
0.5–0.7	Moderate
0.7–0.9	Strong
> 0.9	Very strong

Statistics and data analysis

Pearson correlation analysis

Pearson's correlation analysis assessed the degree of association between the several variables (Table 1). This evaluation followed the organization and compilation of the data set (Mukaka 2012).

Principal component analysis (PCA)

After using Pearson's correlation analysis, the data set was subjected to principal component analysis (PCA). This multivariate statistical technique turns an original set of variables into a new set of variables of the same dimension called principal components (PC) (Wilks 2011). The PC possesses crucial properties: each PC is a linear combination of the original data, is independent of one another, and is estimated to maintain, in a sequence of estimation, the highest information regarding the entire variation in the data (Wilks 2011). In addition, PCA is related to data reduction with minimal information loss.

This reduction was only possible if these variables were interdependent and correlated (Oliveira-Júnior et al. 2021; Costa et al. 2021; Correia Filho et al. 2022b). Therefore, the application of PCA requires evaluating the quality of the data set in this way, using the Kaiser–Meyer–Olkin (KMO) and Measure of Sampling Adequacy (MSA) tests (Kaiser 1970; Kaiser and Rice 1974), obtained by Eqs. 1 and 2:

$$\text{KMO} = \frac{\left(\sum_j \sum_{k \neq j} r_{jk}^2\right)}{\left(\sum_j \sum_{k \neq j} r_{jk}^2 + \sum_j \sum_{k \neq j} p_{jk}^2\right)}, \quad (1)$$

$$\text{MSA} = \frac{\left(\sum_{k \neq j} r_{jk}^2\right)}{\left(\sum_{k \neq j} r_{jk}^2 + \sum_{k \neq j} p_{jk}^2\right)}, \quad (2)$$

where r is the standard correlation coefficient, p is the standard partial correlation coefficient, and the KMO and MSA value ranges from 0 to 1.

According to Corrar et al. (2007), KMO and MSA values below 0.5, the matrix is discarded, whereas values between 0.5 and 0.7 are reasonable, 0.7 and 0.9 are good, and above 0.9 are optimal. The PCA was applied to the data based on the results of the KMO and MSA tests. It identified the optimal number of PC using the Kaiser method, which selects eigenvalues greater than 1 ($\lambda > 1$) (Kaiser 1970) and evaluated the influence of each PC based on its respective factor loading (scores).

Table 2 Correlation analysis (CA) of the variables analyzed for PC1, PC2, and PC3

Variables	KMO	PC1	PC2	PC3
Elevation	0.75	0.49	−0.42	0.58
Evapotranspiration	0.86	−0.67	0.10	−0.37
Active fires	0.84	−0.68	0.39	−0.04
HDI	0.82	0.86	0.04	0.02
LULC—cropland/rainfed	0.79	0.50	0.46	0.28
LULC—shrubland	0.57	0.29	−0.47	−0.69
Autumn rainfall	0.67	0.79	0.51	0.00
Spring rainfall	0.62	0.56	0.68	−0.19
Livestock	0.90	0.56	0.13	−0.23
KMO factor adequacy	Overall MSA = 0.76			

The KMO and MSA tests vary between 0.50 and 1. The CA varies between −1 and 1

Results

The MSA and KMO tests were initially applied to select the matrix dataset based on 17 variables and evaluate the quality. The MSA test presents that only nine meet the minimum requirements for PCA (MSA and KMO tests > 0.50), and the overall matrix has good quality, with a value of 0.76 (Table 2). The variables selected are elevation, evapotranspiration, active fires, HDI, LULC-shrubland, LULC-cropland/rainfed, spring rainfall, autumn rainfall, and livestock, as described in Table 2. In addition, correlation analysis (CA) was applied based on the new data matrix to determine potential relationships between variables (Fig. 2).

The CA matrix showed a moderate positive correlation ($0.39 < CA < 0.69$) between evapotranspiration and active fires (0.40) and autumn rainfall with livestock (0.40). In addition, there is an association of the HDI with other variables such as autumn rainfall (0.67), spring rainfall (0.44), and with livestock (0.41), while the strong positive correlation ($0.70 < CA < 0.89$) between autumn rainfall and spring rainfall (0.77). Regarding the moderate negative correlations, evapotranspiration is associated with other variables such as elevation (0.41), autumn rainfall (0.45), HDI (0.48), and active fires (0.48). In addition, it checks for associations of active fires with other variables such as elevation (0.40) and HDI (0.55) stand out.

After performing CA on the dataset, PCA was used to detect spatial patterns. The variables are categorized as follows based on KMO values: LULC-shrubland as bad ($0.5 < \text{KMO} < 0.6$); spring rainfall and autumn rainfall as reasonable ($0.6 < \text{KMO} < 0.7$); elevation and LULC-cropland/rainfed as average ($0.7 < \text{KMO} < 0.8$); and evapotranspiration, active fires, HDI, and livestock as good ($0.8 < \text{KMO} < 0.9$), with emphasis on the highest values obtained by evapotranspiration (0.86) and livestock

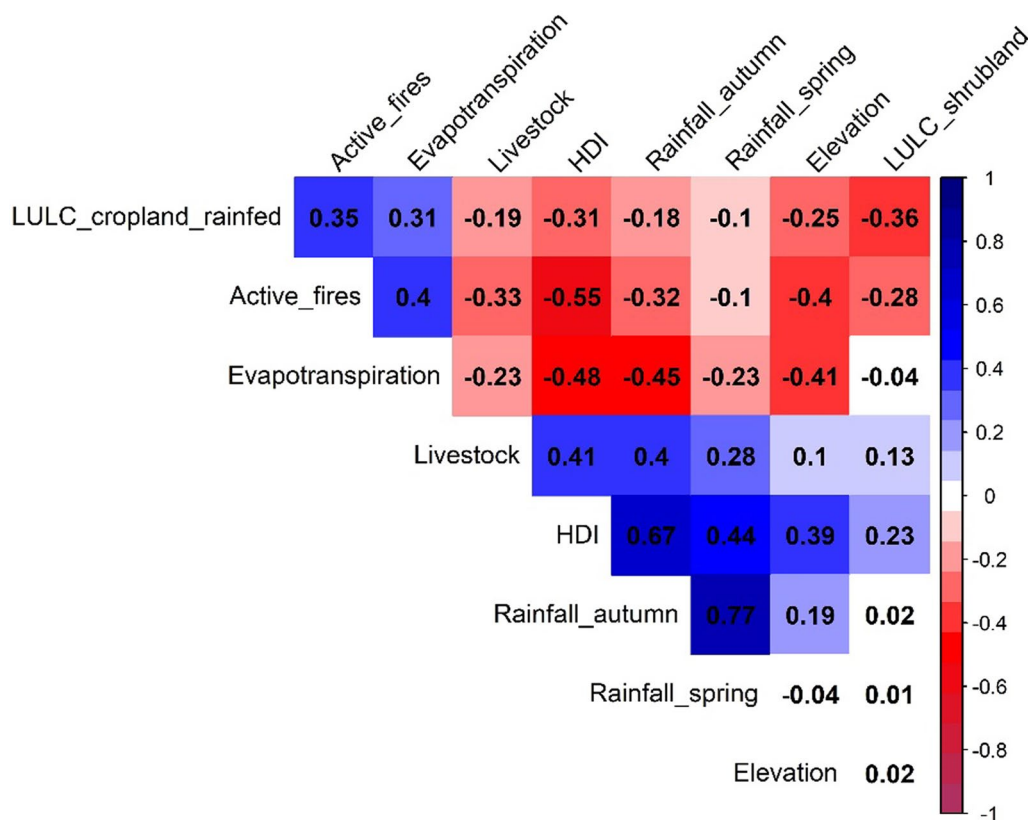


Fig. 2 The Pearson correlation analysis of the nine variables selected by PCA. The highlighted blue (red) square demonstrates a positive (negative) relationship between the variables analyzed. The result is statistically significant ($p < 0.05$), ranging from -1 to 1

Table 3 Contribution percentage (in %) of the variables analyzed for PC1, PC2, and PC3, with their respective to total variance explained (in %)

Variables	PC1	PC2	PC3
Elevation	6.78	11.60	29.81
Evapotranspiration	13.10	0.61	12.36
Active fires	13.35	9.85	0.15
HDI	21.10	0.13	0.04
LULC—cropland/rainfed	7.26	14.24	7.01
LULC—shrubland	2.38	14.47	42.59
Autumn rainfall	17.86	17.32	0.00
Spring rainfall	9.17	30.63	3.29
Livestock	8.99	1.14	4.76
Total of variance explained (%)	38.59	16.87	12.56

The variance explained and contribution percentage vary between 0 and 100

(0.90). Finally, the Kaiser test ($\lambda > 1$) was used to determine the optimal number of principal components (PC), and it noted that three PCs would extract the spatial patterns, explaining 68.02% of the total variance explained (Table 3).

Figure 3 shows the relationships between variables using a biplot graph. HDI and autumn rainfall (livestock and elevation) are the most (minor) representative variables, each accounting for 15% (<7%) of the variance. PC1 accounts for 38.59% of the total variance explained (Table 3 and Fig. 4a), and its positive correlations are greater than 0.29, with highlights for autumn rainfall (0.86), followed by HDI (0.79). On the other hand, negative correlations are observed by evapotranspiration (-0.67) and active fires (-0.68). Regarding the scores (Fig. 4, top right panel), the northern portion of Cerrado (Bahia, Maranhão, and Piauí States) shows negative values between -5 and -10 , whereas the western, central, and southern regions (Goiás, Mato Grosso, Minas Gerais, Mato Grosso do Sul, Paraná, and São Paulo States) show positive scores upper 5.

The results of PC1 exhibit a distinctive characteristic: the dominance of a socioeconomic variable (HDI) over climatological and environmental variables. HDI and autumn rainfall contribute the most (least) to PC1 (Table 3), with respective contributions of 21.10% and 17.86% of the total variance explained (6.78% and 2.38% of the total for elevation and LULC-shrubland, respectively).

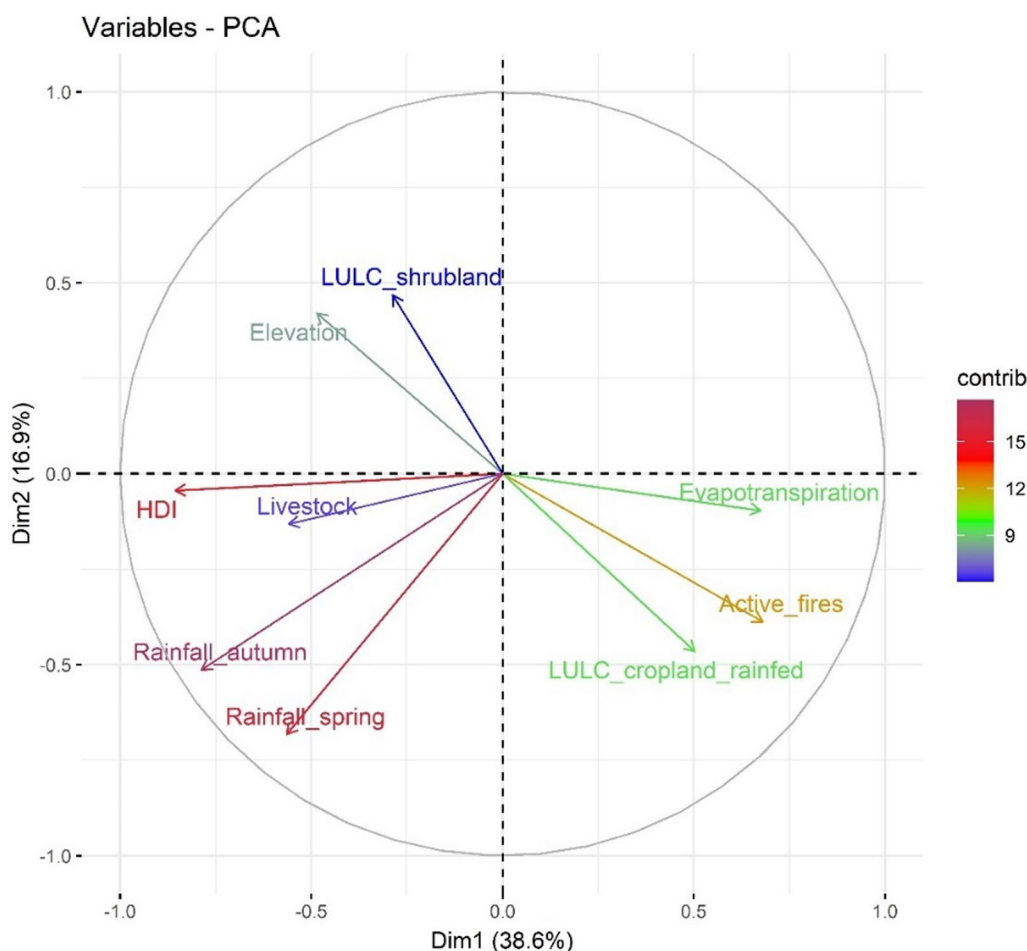


Fig. 3 Biplot resulting from two PC-based PCA. The colors of the arrows represent the contribution (in %) of each variable evaluated for PC1 and PC2 over the Brazilian Cerrado. The x and y axes correspond to the degree of relationship of each PCA resulting correlation analysis. In this instance, x and y refer to PC1 and PC2, respectively. These respective axes' values range from -1 to 1

PC2 accounts for 16.87% of the total explained variance (Fig. 4, top right panel), with most variables in this PC exhibiting positive correlations corresponding to rainfall (spring and autumn with values of 0.68 and 0.51, respectively). However, LULC-shrubland (-0.47) and elevation (-0.42) demonstrate negative correlations. The scores of this PC (Fig. 4, top right panel) exhibit negative (positive) values that vary between -5 and -0.25 (between 0.25 and 5) situated in the northwestern and western portions of the Cerrado over the Mato Grosso and Tocantins States (eastern and southern regions of the Cerrado). The variables contributing the most (least) to PC2 (Table 3) are autumn rainfall and spring rainfall, with 17.32% and 30.63% of the total variance explained, respectively (HDI contributes 0.13% of the total, respectively).

PC3 accounts for 12.56% of the explained variance (Table 3). LULC-shrubland and elevation stand out among the variables examined due to their respective values of -0.69 and 0.58 , respectively. Furthermore,

positive scores (Fig. 4, bottom left panel) are found in the eastern (Bahia, southern Maranhão, northern Minas Gerais, and Piauí States) and western (central region of Mato Grosso State) portions of the Cerrado, with values between 0.25 and 3. In contrast, negative scores occur in the center-southern (Goiás and Mato Grosso do Sul States) and northern (northern Maranhão State) portions of the Cerrado, with values between -3 and -0.25 . As a result, LULC-shrubland and elevation contribute the most (least) to PC3 (Table 3), accounting for 29.81% and 42.51% of the total variance, respectively.

Discussion

The PCA patterns from the three PC indicate distinct characteristics. Checking the relationship patterns exhibited by Pearson's correlation and the respective PCA maps reveals that the HDI (socioeconomic aspect) is the primary variable in PC1 behavior. The HDI is an essential indicator of the development level of a city, region, and

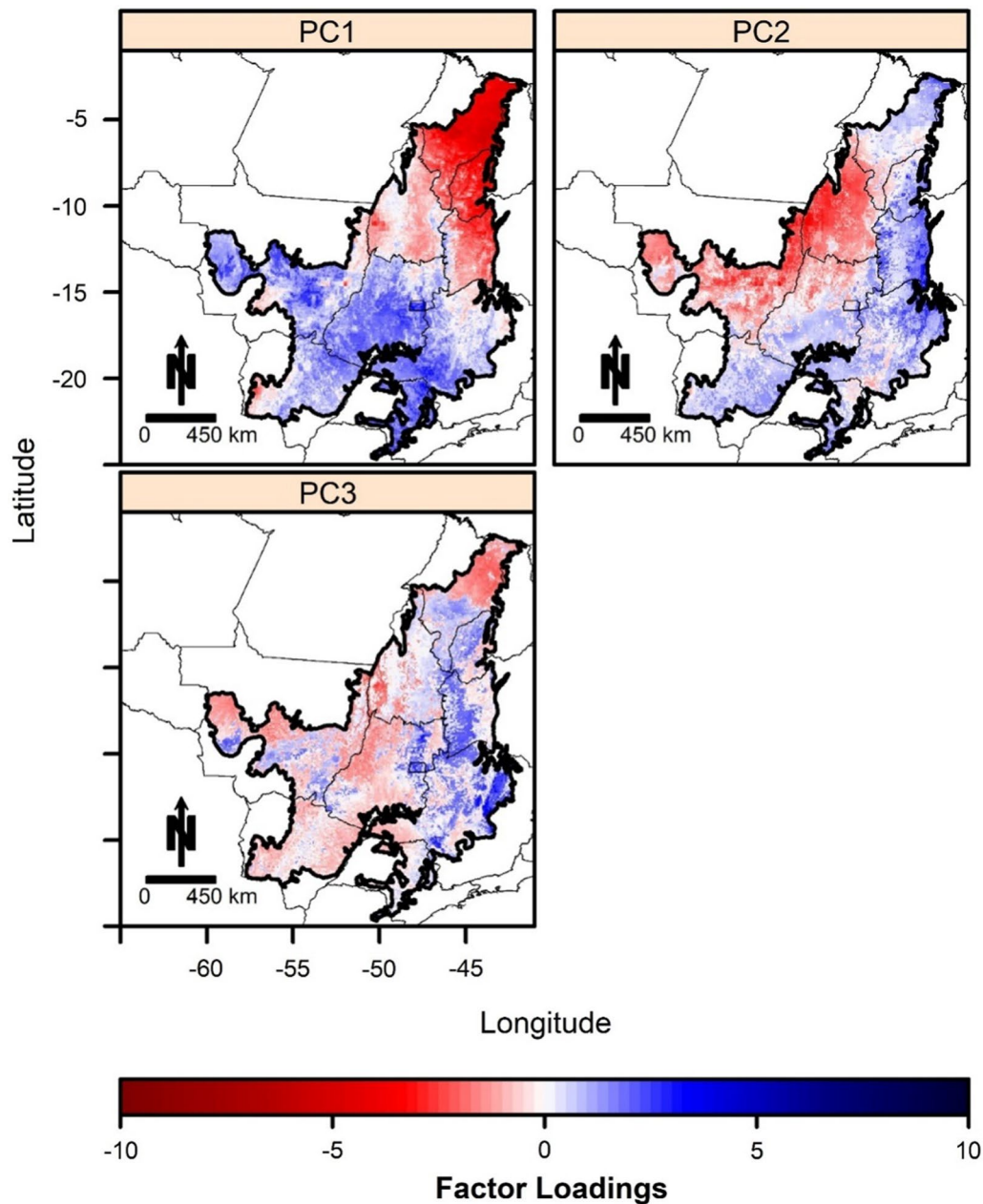


Fig. 4 Spatial factor loadings (scores) corresponding to each of the three PC: PC1 (top left panel), PC2 (top right panel), and PC3 (bottom left panel). The colors represent the influence of each PC's positive (blue) or negative (red). The scores range in value from -10 to 10

country (Santos et al. 2011; Espírito Santo et al. 2016). It is observed that positive scores of the PC1 are associated with the regions of the highest HDI values (central and southern portions of the Cerrado) due to the agricultural development based on agribusiness, the primary sector of the Brazilian production chain (Rocha et al. 2011; Dias et al. 2016; Espírito-Santo et al. 2016; Spangler et al. 2017).

In the southern portion of Cerrado, agricultural cultivation is multifaceted, primarily involving the planting of cotton, corn, soybean, and sorghum (Rocha et al. 2011; Sano et al. 2010; Dias et al. 2016; Magalhães et al. 2020; Oliveira et al. 2021), and in the southeastern portion, sugarcane in Minas Gerais and São Paulo States (Rudorff et al. 2010; Mataveli et al. 2018; Marinho et al. 2021). Soybean production is the source of agricultural expansion in the northern portion of the Cerrado (the agricultural

frontier MATOPIBA). Although this agricultural development benefits the region's economy, its effects generate environmental consequences (Silva et al. 2013; Silva Junior et al. 2018; Picoli et al. 2020). One of these is the significant change in LULC caused by deforestation and the use of fire, corroborating with some studies in Cerrado (Sano et al. 2010; Rocha et al. 2011; Santos et al. 2011; Buainain and Garcia 2015; Picoli et al. 2020; Oliveira et al. 2021).

PC2's behavior is determined by climatic and environmental aspects based on rainfall (spring and autumn) and LULC (LULC-cropland/rainfed and LULC-shrubland). The transition zones influenced this pattern of negative scores with the Amazon biome (to the western Cerrado), which has a humid and warm environment with high rainfall rates ranging from 2000 to 3000 mm year⁻¹ from the Amazon Forest (Silva Junior et al. 2019).

Regarding climatic conditions, rainfall (spring and autumn) is essential for crop development during the planting (mid-November) and harvesting (late May) periods, respectively (Sprangler et al. 2017). However, irregular rainfall patterns can imperil the cultivation phases and reduce crop yield (Dias et al. 2016; Soterroni et al. 2019). Therefore, planting occurs during the Cerrado's rainy period, which begins in September and lasts until mid-May (Campos and Chaves 2020; Oliveira-Júnior et al. 2021; Correia Filho et al. 2022a), as a result of the South American Monsoon System (SAMS), which initiates and maintains the South Atlantic Convergence Zone (Reboita et al. 2010; Nielsen et al. 2016; Correia Filho et al. 2022a).

Campos and Chaves (2020) reported a negative trend of an 8% decline in annual rainfall totals over the Cerrado. The authors assume that this drop in rainfall results from the weakening of the SACZ, the system responsible for the rainy season, and that its variability threatens the growth of non-irrigated crops. In addition, this drop in rainfall occurs across the depressions of the lower and middle Araguaia and the Araguaia River Plain/Bananal Island (elevation < 300 m), where shrubland/wetland vegetation predominates (Sano et al. 2020).

According to Sprangler et al. (2017), Campos and Chaves (2020), and Nascimento and Novais (2020), the northern and eastern portions (regions with negative scores)—also known as the transition zone between Cerrado–Caatinga with a semi-arid climate and low rainfall regimes (700–1000 mm year⁻¹)—have the lowest rainfall rates (Correia Filho et al. 2019; Correia Filho et al. 2022a). Therefore, this location offers ideal circumstances for promoting evapotranspiration and the emergence of active fires.

Santos et al. (2020) examined Cerrado's annual potential evapotranspiration (ETp) in the Brazilian Northeast from 1979 to 2013. The authors detected that the greatest

annual ETp rates occurred in Maranhão and Piauí States. This decrease in rainfall mentioned earlier, coupled with high ETp rates, contributes to increased plant/crop stress and, consequently, to the loss of vegetation cover (Correia Filho et al. 2018). Rocha et al. (2011), Santos et al. (2014), Soterroni et al. (2019), Souza et al. (2020b), and Oliveira et al. (2021) found that these climatic and environmental circumstances, in conjunction with land-use changes, have contributed to the wildfires in the region, notably between the Maranhão and Tocantins States.

According to Oliveira et al. (2021), this combination of elements may contribute to the elevated springtime fire risk in the aforementioned regions (September–October–November). Santos et al. (2014) analyzed the pattern of active fire over the Cerrado from 2002 to 2014. The authors discovered that the highest active fire concentrations found in Maranhão, Piauí, and Tocantins States are related to the expansion of the MATOPIBA agricultural frontier (Rocha et al. 2011). In this extension, agricultural concentrations occur precisely in deforested and eroding regions, including Bahia (Assis et al. 2021). In addition, the LULC may be related to agricultural production based in the commodities and the cattle industry expansion, situated in Goiás, Minas Gerais, and Mato Grosso States (Cunha et al. 2008; Silva et al. 2013; Dias et al. 2016), to which they are responsible for the production of animal protein for export.

Already, PC3's behavior exhibits environmental aspects as main responsible. In Maranhão State, low-elevation regions (< 300 m) have negative scores distributed intermittently over the Coastal, Cocais Forest (Tabuleiros de Barreirinhas and Bacabal Surface), and Bico do Papagaio ecoregions. Moreover, Tocantins contains the lower and middle Araguaia depressions and the Araguaia River Plain/Bananal Island (Sano et al. 2020). Santos et al. (2020) assessed the ETp over Brazilian Northeast (northern portion of the Cerrado), and discovered that northern Maranhão (region with low-elevation, < 300 m) had the highest evapotranspiration values, with values exceeding 1250–2000 mm year⁻¹, while Bahia (region with elevation > 800 m) presented values ranging from 600 to 1500 mm year⁻¹. This behavior presented by ETp displays the importance of the elevation gradient, to which the measure that increases the elevation, there is a decrease in air temperature and relative humidity of the air, to which both contribute to the decrease of the processes inherent in ETp, corroborating with Goulden et al. (2012) to which they assessed the behavior of the ETp over the Sierra Nevada in California, USA.

Conclusions

According to the results, nine variables (elevation, evapotranspiration, active fires, HDI, LULC-shrubland, LULC-cropland/rainfed, spring rainfall, autumn rainfall, and livestock) were sufficient for understanding some aspects of the Brazilian Cerrado. Based on the correlation matrix, it was verified that the positive correlations between HDI and autumn rainfall occurred in the agribusiness regions (central and southern portions of the biome). In addition, the results demonstrated a negative association between HDI and active fires in areas with low (high) HDI values, which had a high (low) active fire rate due to the expansion and development of agriculture and cattle-raising. This high frequency of active fires contributes to deforestation along the MATOPIBA agricultural frontier, driven by changes in LULC.

The PCA results revealed three distinct patterns. The PC1 highlighted by the HDI and the autumn rainfall being two more representative variables with positive scores in Cerrado's central, western, and southern portions. HDI is the most significant socioeconomic indicator that represents the growth of a city, region, or country and is conditioned to climatological, environmental, and socioeconomic variables. The higher HDI is located in agribusiness regions, the most significant industry in the production chain of the Brazilian economy.

The most influential climatological and environmental variables for PC2 were rainfall (spring and autumn) and LULC (cropland/rainfed and shrubland). Due to this seasonal rainfall pattern (LULC), Cerrado's eastern and southern regions presented negative (positive) score values. This negative score pattern is influenced by the transition region between the Amazon and Cerrado biomes (to the west) due to the irregularity of the rainfall regime. This variability in rainfall during the spring contributes to the increased risk of wildfires along the biome.

The PC3 emphasized climatological and environmental data, highlighting the LULC-shrubland, elevation, and evapotranspiration as the most important. In the eastern and western Cerrado, positive scores were obtained in regions with LULC-shrubland or high-elevation areas (>500 m), while the negative scores are dispersed periodically along the Cerrado for low-elevation regions with high evapotranspiration levels in northern Maranhão and Tocantins.

Acknowledgements

The authors thank CNPq and CAPES (Financial Code 001) for their scholarship awards. This article was developed during the Post-Doctorate Junior scholarship of no. 161023/2019-3 granted by Brazilian National Council for Scientific and Technological Development (CNPq) at the first author. The second author thanks CNPq for granting the Research Productivity Fellowship level 2 (309681/2019-7).

Author contributions

WLFCF: methodology, WLFCF, and DBS: software and data curation, WLFCF, JFOJ, and DBS: formal analysis and investigation. WLFCF and DBS: visualization, WLFCF: writing—original draft preparation, JFOJ; DBS, CASJ, HGA, AAA, and HA: writing—review and editing, CASJ and JFOJ: supervision. All authors have agreed to the published version of the manuscript. All authors read and approved the final manuscript.

Funding

Not applicable.

Data availability

This research work is part of the Post-Doctorate Junior of the first author. The data are available on request to the first author.

Declarations

Ethics approval and consent to participate

This article does not contain any studies with human participants or animals performed by any of the authors.

Consent for publication

Not applicable.

Competing interests

The authors declare that they have no known competing financial interests or personal relationships that could have appeared to influence the work reported in this paper.

Author details

¹Postgraduate Program in Environmentrics (PPGAmb), Institute of Mathematics, Statistics, and Physics (IMEF), Federal University of Rio Grande (FURG), Rio Grande, Rio Grande do Sul 96203-900, Brazil. ²Institute of Atmospheric Sciences (ICAT), Federal University of Alagoas (UFAL), Maceió, Alagoas 57072-260, Brazil. ³Postgraduate Program in Biosystems Engineering (PGEB), Federal Fluminense University (UFF), Niterói, Rio de Janeiro 24220-900, Brazil. ⁴Postgraduate Program in Meteorology, Unidade Acadêmica de Ciências Atmosféricas (UACA), Federal University of Campina Grande (UFCG), Campina Grande, Paraíba 58429-140, Brazil. ⁵Geography Department, Faculty of Arts and Humanities, Tartous University, Tartous, Syria. ⁶Geography Department, Faculty of Arts and Humanities, Damascus University, Damascus, Syria. ⁷Geography Department, Faculty of Arts and Humanities, Tishreen University, Latakia, Syria. ⁸Department of Geography, College of Arabic Language and Social Studies, Qassim University, Buraydah 51452, Saudi Arabia. ⁹Departamento de Geografia, State University of Mato Grosso (UNEMAT), Sinop, Mato Grosso 78555-000, Brazil.

Received: 6 December 2022 Accepted: 31 March 2023

Published online: 19 April 2023

References

- Abdo HG (2018) Impacts of war in Syria on vegetation dynamics and erosion risks in Safita area, Tartous, Syria. *Reg Environ Change* 18(6):1707–1719. <https://doi.org/10.1007/s10113-018-1280-3>
- Abdo HG, Almohamad H, Al Dughairi AA, Al-Mutiry M (2022) GIS-based frequency ratio and analytic hierarchy process for forest fire susceptibility mapping in the western region of Syria. *Sustainability* 14(8):4668. <https://doi.org/10.3390/su14084668>
- Abreu RCR, Hoffmann WA, Vasconcelos HL, Pilon NA, Rossatto DR, Durigan G (2017) The biodiversity cost of carbon sequestration in tropical savanna. *Sci Adv* 3(8):e1701284. <https://doi.org/10.1126/sciadv.1701284>
- Alves PJP, Rosa O (2019) Consciência ecológica na escola: um estudo de caso sobre o ensino - aprendizagem do bioma cerrado na escola pública. *Revista Eixo* 8(2):150–155
- Assis TO, Escada MIS, Amaral S (2021) Effects of deforestation over the Cerrado landscape: a study in the Bahia frontier. *Land* 10(4):352. <https://doi.org/10.3390/land10040352>

- Becerra JAB, Shimabukuro YE, Santos Alvalá RC (2009) Relação do padrão sazonal da vegetação com a precipitação na região de cerrado da Amazônia Legal, usando índices espectrais de vegetação. *Revista Brasileira de Meteorologia* 24(2):125–134. <https://doi.org/10.1590/S0102-77862009000200002>
- Bontemps S, Boettcher M, Brockmann C et al (2015) Multi-year global land cover mapping at 300 m and characterization for climate modelling: achievements of the land cover component of the ESA climate change initiative. *ISPRS Arch* 40:323–328. <https://doi.org/10.5194/isprsarchives-XL-7-W3-323-2015>
- Buainain AM, Garcia JR (2015) Evolução recente do agronegócio no cerrado nordestino. *Estudos Sociedade e Agricultura* 23(1):166–195
- Campos JO, Chaves HML (2020) Tendências e Variabilidades nas Séries Históricas de Precipitação Mensal e Anual no Bioma Cerrado no Período 1977–2010. *Revista Brasileira de Meteorologia* 35(1):157–169. <https://doi.org/10.1590/0102-7786351019>
- Corrar LJ, Paulo E, Dias Filho JM (2007) Análise Multivariada - Para os Cursos de Administração, Ciências Contábeis e Economia. Atlas, São Paulo, p 344
- Correia Filho WLF, dos Santos TV, Diogo AM, de Amorim RFC (2018) Diagnóstico da Precipitação e EVI em Dois Eventos de Seca no Nordeste do Brasil. *Revista do Departamento de Geografia* 35:102–112. <https://doi.org/10.11606/rdg.v35i0.140068>
- Correia Filho WLF, De Oliveira-Júnior JF, Santiago DD et al (2019) Rainfall variability in the Brazilian northeast biomes and their interactions with meteorological systems and ENSO via CHELSA product. *Big Earth Data* 3(4):315–337. <https://doi.org/10.1080/20964471.2019.1692298>
- Correia Filho WLF, de Oliveira-Júnior JF, da Silva Junior CA, Santiago DB (2022a) Influence of the El Niño–Southern oscillation and the synoptic systems on the rainfall variability over the Brazilian Cerrado via Climata Hazard Group InfraRed precipitation with station data. *Int J Climatol* 42(6):3308–3322. <https://doi.org/10.1002/joc.7417>
- Correia Filho WLF et al (2022b) The influence of urban expansion in the socioeconomic, demographic, and environmental indicators in the City of Arapiraca–Alagoas, Brazil. *Remote Sens Appl Soc Environ* 25:100662. <https://doi.org/10.1016/j.rsase.2021.100662>
- Costa JC, Pereira G, Siqueira ME, da Silva Cardozo F, Da Silva VV (2019) Validação dos Dados de Precipitação Estimados pelo CHIRPS para o Brasil. *Revista Brasileira de Climatologia*. <https://doi.org/10.5380/abclima.v24i0.60237>
- Costa MDS, Oliveira-Júnior JFD, Santos PJD, Correia Filho WLF, Gois GD, Blanco CJC, Teodoro PE, Silva Junior CA, Santiago DB, Souza EO, Jardim AMRF (2021) Rainfall extremes and drought in Northeast Brazil and its relationship with El Niño–Southern Oscillation. *Int J Climatol* 41:E2111–E2135. <https://doi.org/10.1002/joc.6835>
- CPTEC/INPE - Centro de Previsão de Tempo e Estudos Climáticos/Instituto Nacional de Pesquisas Espaciais (2019) Portal do Monitoramento de Queimadas e Incêndios. www.sigma.cptec.inpe/queimadas. Accessed 15 Nov 2020
- Cunha NRDS, Lima JED, Gomes MFD, Braga MJ (2008) A intensidade da exploração agropecuária como indicador da degradação ambiental na região dos Cerrados, Brasil. *Rev Econ Sociol Rural* 46(2):291–323. <https://doi.org/10.1590/S0103-20032008000200002>
- Dias LC, Pimenta FM, Santos AB, Costa MH, Ladle RJ (2016) Patterns of land use, extensification, and intensification of Brazilian agriculture. *Glob Change Biol* 22(8):2887–2903. <https://doi.org/10.1111/gcb.13314>
- Durigan G, Ratter JA (2016) The need for a consistent fire policy for Cerrado conservation. *J Appl Ecol* 53(1):11–15. <https://doi.org/10.1111/1365-2664.12559>
- ESA—European Space Agency (2021) Climate change initiative, land cover maps—v2.0.7, land covers maps 2000 and 2015. https://storage.googleapis.com/ccci-ic-v207/ESACCI-LC-L4-LCCS-Map-300m-P1Y-1992_2015-v2.0.7.zip. Accessed 01 Mar 2021
- Espirito-Santo MM, Leite ME, Silva JO, Barbosa RS, Rocha AM, Anaya FC, Dupin MG (2016) Understanding patterns of land-cover change in the Brazilian Cerrado from 2000 to 2015. *Philos Trans R Soc B Biol Sci* 371(1703):20150435. <https://doi.org/10.1098/rstb.2015.0435>
- Funk C, Peterson P, Landsfeld M, Pedreros D, Verdin J, Shukla S, Husak G, Rowland J, Harrison L, Hoell A, Michaelsen J (2015a) The climate hazards infrared precipitation with record for monitoring extremes. *Sci Data* 2(1):10–66. <https://doi.org/10.1038/sdata.2015.66>
- Funk C, Verdin A, Michaelsen J, Peterson P, Pedreros D, Husak GA (2015b) Global satellite-assisted precipitation climatology. *Earth Syst Sci Data* 7(2):275–287. <https://doi.org/10.5194/essd-7-275-2015b>
- Garcia AS, Ballester MVR (2016) Land cover and land use changes in a Brazilian Cerrado landscape: drivers, processes, and patterns. *J Land Use Sci* 11(5):538–559. <https://doi.org/10.1080/1747423X.2016.1182221>
- Goldemberg J, Lucon O (2007) Energia e meio ambiente no Brasil. *Estudos Avançados* 21(59):7–20. <https://doi.org/10.1590/S0103-40142007000100003>
- Goulden ML, Anderson RG, Bales RC, Kelly AE, Meadows M, Winston GC (2012) Evapotranspiration along an elevation gradient in California's Sierra Nevada. *J Geophys Res Biogeosci* 117:G03028. <https://doi.org/10.1029/2012JG002027>
- Grupo de Trabalho Do Bioma Cerrado (2004) Programa Nacional de Conservação e Uso Sustentável do Bioma Cerrado. http://cerradobrasil.cpac.embrapa.br/prog%20cerrado%20sust_ent.pdf. Accessed 02 Mar 2021
- Hunke P, Mueller EN, Schröder B, Zeilhofer P (2015) The Brazilian Cerrado: assessment of water and soil degradation in catchments under intensive agricultural use. *Ecohydrology* 8(6):1154–1180. <https://doi.org/10.1002/eco.1573>
- IIASA/FAO—International Institute for Applied Systems Analysis/Food and Agriculture Organization (2012) Global agro-ecological zones (GAEZ v3.0). IIASA, Laxenburg, Austria and FAO, Rome
- Jarvis A, Reuter HI, Nelson A, Guevara E (2008) Hole-filled SRTM for the globe Version 4, available from the CGIAR-CSI SRTM 90m Database. <http://srtm.csi.cgiar.org>
- Kaiser HF (1970) A second generation little jiffy. *Psychometrika* 35(4):401–415. <https://doi.org/10.1007/BF02291817>
- Kaiser HF, Rice J (1974) Little jiffy, mark IV. *Educ Psychol Meas* 34(11):111–117. <https://doi.org/10.1177/001316447403400115>
- Karnieli A et al (2010) Use of NDVI and land surface temperature for drought assessment: merits and limitations. *J Clim Am Meteorol Soc* 24:618–633. <https://doi.org/10.1175/2009JCLI2900.1>
- Kogan F, Guo W, Jelenak A (2011) Global vegetation health: long-term data records. Use of satellite and in-situ data to improve sustainability. Springer, Dordrecht, pp 247–255. https://doi.org/10.1007/978-90-481-9618-0_28
- Kummu M, Taka M, Guillaume JH (2018) Gridded global datasets for gross domestic product and Human Development Index over 1990–2015. *Sci Data* 5(1):1–15. <https://doi.org/10.1038/sdata.2018.4>
- Magalhães IB, de Paula Pereira ASA, Calijuri ML, do Carmo Alves S, dos Santos VJ, Lorentz JF (2020) Brazilian Cerrado and Soy moratorium: effects on Biome preservation and consequences on grain production. *Land Use Policy* 99:105030. <https://doi.org/10.1016/j.landusepol.2020.105030>
- Marinho AAR, de Gois G, de Oliveira JF et al (2021) Temporal record and spatial distribution of fire foci in State of Minas Gerais, Brazil. *J Environ Manag* 280:111707. <https://doi.org/10.1016/j.jenvman.2020.111707>
- Mataveli GAV, Silva MES, Pereira G et al (2018) Satellite observations for describing fire patterns and climate-related fire drivers in the Brazilian savannas. *Nat Hazard Earth Syst Sci* 18(1):125–144. <https://doi.org/10.5194/nhess-18-125-2018>
- Mukaka MM (2012) A guide to appropriate use of correlation coefficient in medical research. *Malawi Med J* 24(3):69–71
- Nascimento D, Novais G (2020) Clima do Cerrado: dinâmica atmosférica e características, variabilidades e tipologias climáticas. *Élisée - Revista De Geografia Da UEG* 9(2):e922021
- Nielsen DM, Cataldi M, Belém AL, Albuquerque ALS (2016) Local indices for the South American monsoon system and its impacts on Southeast Brazilian precipitation patterns. *Nat Hazards* 83:909–928. <https://doi.org/10.1007/s11069-016-2355-4>
- Oliveira U, Soares-Filho B, de Souza Costa WL, Gomes L, Bustamante M, Miranda H (2021) Modeling fuel loads dynamics and fire spread probability in the Brazilian Cerrado. *For Ecol Manag* 482:118889. <https://doi.org/10.1016/j.foreco.2020.118889>
- Oliveira-Júnior JF, da Silva CA, Teodoro PE et al (2021) Confronting CHIRPS dataset and in situ stations in the detection of wet and drought conditions in the Brazilian Midwest. *Int J Climatol* 41:4478–4493. <https://doi.org/10.1002/joc.7080>
- Palharini RSA, Vila DA, Rodrigues DT, Palharini RC, Mattos EV, Pedra GU (2021) Assessment of extreme rainfall estimates from satellite-based: regional

- analysis. *Remote Sens Appl Soc Environ* 23:100603. <https://doi.org/10.1016/j.rsase.2021.100603>
- Picoli MC, Rorato A, Leitão P, Camara G, Maciel A, Hostert P, Sanches IDA (2020) Impacts of public and private sector policies on soybean and pasture expansion in Mato Grosso—Brazil from 2001 to 2017. *Land* 9(1):20. <https://doi.org/10.3390/land9010020>
- R Development Core Team (2020) R: a language and environment for statistical computing. R Foundation for Statistical Computing, Vienna, Austria. <https://cran.r-project.org/bin/windows/base/old/3.6.3/>
- Reboita MS, Gan MA, Rocha RP, Ambrizzi T (2010) Regimes de precipitação na América do Sul: uma revisão bibliográfica. *Rev Bras Meteorol* 25:185–204. <https://doi.org/10.1590/S0102-77862010000200004>
- Rocha GF, Ferreira LG, Ferreira NC, Ferreira ME (2011) Detecção de desmatamentos no bioma Cerrado entre 2002 e 2009: padrões, tendências e impactos. *Rev Bras Cartogr* 63(3):341–349
- Rudorff BFT, de Aguiar DA, da Silva WF et al (2010) Studies on the rapid expansion of sugarcane for ethanol production in São Paulo state (Brazil) using Landsat data. *Remote Sens* 2:1057–1076. <https://doi.org/10.3390/rs2041057>
- Running S, Mu Q, Zhao M (2017) MOD16A2 MODIS/Terra net evapotranspiration 8-day L4 global 500m SIN grid V006 [01-01-2001 to 12-31-2020]. NASA EOSDIS land processes DAAC. <https://doi.org/10.5067/MODIS/MOD16A2.006>. Accessed 04 July 2021
- Salazar Pessoa V (2020) O paradoxo da Revolução Verde no Cerrado. *Élisée - Revista De Geografia Da UEG* 9(2):e922013
- Sano EE, Rosa R, Brito JL, Ferreira LG (2010) Land cover mapping of the tropical Savanna region in Brazil. *Environ Monit Assess* 166(1):113–124. <https://doi.org/10.1007/s10661-009-0988-4>
- Sano EE, Bettiol GM, Martins EDS, Couto Júnior AF, Vasconcelos V, Bolfe EL, Victoria DDC (2020) Características gerais da paisagem do Cerrado. Embrapa Informática Agropecuária-Capítulo em livro científico (ALICE)
- Santos NBF, Júnior LGF, Ferreira NC (2011) Caracterização Socioeconômica do Cerrado. *Ateliê Geográfico* 5(1):283–292
- Santos PR, Pereira G, Rocha LC (2014) Análise da distribuição espacial dos focos de queimadas para o bioma Cerrado (2002–2012). *Caderno de Geografia* 24(1):133–142
- Santos CB, Correia Filho WLF, Batista BA, Oliveira-Júnior JF, Santiago DB (2020) Estimativa da Evapotranspiração Potencial para o Cerrado Nordestino Brasileiro. *Meteorologia e Recursos Naturais: Estudos Aplicados*. EDUFMG, Campina Grande, pp 350–356
- Silva EB, Júnior LGF, dos Anjos AF, Mizziara F (2013) Análise da distribuição espaço-temporal das pastagens cultivadas no bioma Cerrado entre 1970 e 2006. *RevistaDeAS* 7(1):174–209
- Silva Junior CHL, Anderson LO, Oliveira LE, de Aragão C, Rodrigues BD (2018) Dinâmica das Queimadas no Cerrado do Estado do Maranhão, Nordeste do Brasil. *Revista Do Departamento De Geografia* 35:1–14. <https://doi.org/10.11606/rdg.v35i0.142407>
- Silva Junior CA, Costa GD, Rossi FS et al (2019) Remote sensing for updating the boundaries between the Brazilian Cerrado-Amazonia biomes. *Environ Sci Policy* 101:383–392. <https://doi.org/10.1016/j.envsci.2019.04.006>
- Soteroni AC, Ramos FM, Mosnier A et al (2019) Expanding the soy moratorium to Brazil's Cerrado. *Sci Adv* 5(7):eaav7336. <https://doi.org/10.1126/sciadv.aav7336>
- Souza J, Martins P, Druciaki V (2020a) Uso e cobertura do solo no Cerrado: panorama do período de 1985 a 2018. *Élisée - Revista De Geografia Da UEG* 9(2):e922020
- Souza AA, Galvão LS, Korting TS, Prieto JD (2020b) Dynamics of savanna clearing and land degradation in the newest agricultural frontier in Brazil. *GISci Remote Sens* 57:965–984. <https://doi.org/10.1080/15481603.2020.1835080>
- Spangler KR, Lynch AH, Spera SA (2017) Precipitation drivers of cropping frequency in the Brazilian Cerrado: evidence and implications for decision-making. *Weather Clim Soc* 9(2):201–213. <https://doi.org/10.1175/WCAS-D-16-0024.1>
- Valadão RM, De Brito ES, Helena S, Teixeira S, Silva P (2017) Distribuição de quelônios no Cerrado brasileiro. *Multi-Sci J* 8(1):32
- Wilks DS (2011) *Statistical methods in the atmospheric sciences*, 3rd edn. Elsevier, Philadelphia, p 704

Publisher's Note

Springer Nature remains neutral with regard to jurisdictional claims in published maps and institutional affiliations.

Submit your manuscript to a SpringerOpen® journal and benefit from:

- Convenient online submission
- Rigorous peer review
- Open access: articles freely available online
- High visibility within the field
- Retaining the copyright to your article

Submit your next manuscript at ► [springeropen.com](https://www.springeropen.com)